Ultrasonic Cole-Cole diagram for solutions and application to α-chymotrypsin

Roger Cerf, Seyed-Taghi Salehi, and Daniel Rogez
Laboratoire de Spectrométrie et d'Imagerie Ultrasonores, Unité Associée au Centre National de la Recherche Scientifique, Université Louis Pasteur, 67070 Strasbourg, France

ABSTRACT Deconvolution of ultrasonic data into single relaxations is rarely feasible when only the absorption or the velocity of the waves is measured. Here we use both series of data to construct a Cole-Cole diagram for a solution. When applied to α-chymotrypsin, this method shows two relaxations that are well separated on the time scale, a result that will help simplify analyses of the ultrasonic data for this enzyme.

INTRODUCTION

The simultaneous exploitation of ultrasonic absorption and velocity data described here was stimulated by recent work with biological molecules and supramolecular assemblies. Among the results of interest are: (*a*) the observation in viruses and viral capsids of relaxation effects that are specific to the assembled system (1–4); (*b*) the observation in α-chymotrypsin of an ultrasonic absorption that is large at neutral pH (5), contrary to most known absorption effects in proteins, whose peak values occur at acidic or basic pH.

In the experiments with viruses, the ultrasonic absorption was larger in the tobacco mosaic virus protein helical aggregate than in smaller aggregates by a factor of 4 throughout the frequency range investigated (3,4); this result, and the fact that no dependence of the ultrasonic absorption on pH was found, were interpreted in terms of enhanced volume fluctuations taking place in the helical protein aggregate (4). In the experiments with α-chymotrypsin the ultrasonic absorption was larger in the enzyme than in the zymogen and in the inhibited enzyme, by factors of 8 and 3 respectively. These results led to the conclusion that a proton-transfer reaction involving the histidine at the catalytic site is the primary source for the ultrasonic relaxation in α-chymotrypsin at neutral pH (5).

Deconvolution of a spectrum into single relaxation processes was not a primary objective here, since different states of assembly, or different conformations of a molecule, were compared with each other. It would, nevertheless, be valuable in these experiments to be able to determine the relaxation frequencies and amplitudes. This is obviously not feasible in ultrasonic experiments when only the absorption or only the velocity of the waves is measured over little more than a decade in frequency, except possibly in particular instances when strong arguments exist for postulating a single relaxation process in the frequency range investigated.

Clearly, it is advantageous to measure both the velocity of the ultrasonic waves and their absorption. However, the advantage to be gained is more than just that two quantities are measured instead of only one. This follows because velocity measurements gain in sensitivity relative to absorption measurements as the frequency is increased, whereas the opposite is true when the frequency is decreased. For a single relaxation process, using the symbol δ_N for the change of a measurable over a given frequency interval, the change in velocity, $\delta_N c$, and the change in absorption divided by the square of the frequency, $\delta_N(\alpha/N^2)$, are related by this equation (reference 6):

$$-\frac{\delta_N c}{c^2} = \frac{N_r}{2\pi}\delta_N\left(\frac{\alpha}{N^2}\right), \quad (1)$$

where N_r is the relaxation frequency. For a dilute solution, the velocity c in the denominator of the left hand side of Eq. 1 is practically equal to the value c_0 of c in the solvent. It is seen that $\delta_N c$ increases in absolute value relative to $\delta_N(\alpha/N^2)$ when the relaxation frequency is increased.

High frequency relaxation effects were, indeed, characterized using velocity measurements under conditions in which no relaxation can even be observed using absorption measurements. An example is provided by solutions of polystyrene (7) for which the velocity was found to be molecular-weight-dependent above 30 MHz, i.e., in a frequency-range where the excess absorption due to the solute is too small to be measured.

The object here is to show, using both ultrasonic absorption and velocity measurements, that in α-chymotrypsin at neutral pH the ultrasonic relaxation observed in the megahertz range is well separated from other processes, and can therefore be characterized using absorption measurements only.

0006-3495/89/04/649/06 $2.00

SIMULTANEOUS EXPLOITATION OF ULTRASONIC ABSORPTION AND VELOCITY DATA FOR SOLUTIONS

Either spectrum (the velocity or the absorption) can in principle be obtained from the other by using the Kramers-Kronig relationships. In practice, however, this operation requires data extending from nearly zero to nearly infinite frequency. If data are available only in a restricted frequency range, the transformation of one spectrum into the other is not model-independent. To operate the transformation, one must know the relaxation characteristics, i.e., the actual relaxation frequencies and amplitudes one is looking for.

On the contrary, by using the Cole-Cole representation (8), in which the absorption is plotted against the velocity, both series of data are combined together in a single diagram, the only requirement being that the velocity and the absorption at infinite frequency have been either measured or determined by extrapolation.

The principle of plotting the imaginary part of a measurable quantity against its real part was first used by Cole and Cole in studies of dielectric relaxation, and by Casimir, et al. (9) in studies of paramagnetic relaxation. In each case, including ultrasonic spectroscopy, the relaxation equations provide a parametric representation of the Cole-Cole curve. The parametric variable is $\omega\tau$, in which ω is the circular frequency and τ is a relaxation time. When the process consists of a series of discrete relaxations, τ may be one of the relaxation times; when the process consists of a continuous distribution of relaxations, τ may be some mean relaxation time.

The parametric variable $\omega\tau$ may be varied by changing the frequency ω, and, in principle, also by changing the relaxation time τ, e.g., by varying the temperature. There is, however, in the latter procedure an obvious risk that the relaxation spectrum may be affected by the change of temperature.

Ultrasonic Cole-Cole diagrams were obtained by Kneser for gaseous oxygen, from measurements at different frequencies and pressures P, using the reduced variable N/P (10,11). Ultrasonic Cole-Cole diagrams for liquids were obtained by Sette and Litovitz for glycerol (12) and by Labbardt and Schwarz (13) for an aqueous solution of imidazole and maleic acid. In the work on glycerol, the small number of ultrasonic data available as a function of frequency did not allow for analysis based on variation of ω, and only the temperature variation was used. In Labbardt and Schwarz's work, the variable plotted on the abscissa is twofold too small (compare with Eqs. 10 and 11), so that either paper (13) contains a printing error, or the occurrence of a half-circle in the Cole-Cole plot must be spurious.

In preparation for the study of an enzyme in the next section, the Cole-Cole procedure is here adapted to the analysis of data for solutions. In order to take advantage of the sensitivity of differential measurements of the velocity at high-frequency, we used the excess compressibility β over its high-frequency value β_∞:

$$\delta\beta = \beta - \beta_\infty = \delta\left(\frac{1}{\rho c^2}\right) - \frac{2i\omega}{\rho c}\,\delta\left(\frac{\alpha}{\omega^2}\right), \tag{2}$$

rather than the excess of β over its zero-frequency value β_0. In Eq. 2, ρ is the density of the liquid and $i = \sqrt{-1}$. With the exception of ΔV in Eq. 5, δ and Δ are used for the excess of a measurable quantity over its high-frequency value and over its value in the pure solvent, respectively.

For a single-relaxation process, the excess compressibility at the frequency ω is:

$$\delta\beta = \frac{\beta_0 - \beta_\infty}{1 + i\omega\tau}, \tag{3}$$

where τ is the relaxation time. By virtue of the fluctuation-dissipation theorem, ultrasonic relaxation experiments provide a measurement of the fluctuations of the system (14). For the excess compressibility produced by the solute we thus set:

$$\Delta\beta_0 - \Delta\beta_\infty = \frac{c_M S}{kT}, \tag{4}$$

where c_M is the number of molecules per unit volume, k is Boltzmann's constant, T is the absolute temperature, and S is related to the chemical fluctuations. For example, for a unimolecular process, if there are μ identical independent two-state relaxing systems per molecule, in an aqueous medium, S is the sum of volume fluctuations per molecule (14):

$$S = \mu(\Delta V)^2 \frac{K}{(1+K)^2} \tag{5}$$

and is proportional to the square of the reaction volume ΔV; K is the equilibrium constant.

When the solvent is nonrelaxing we have:

$$\delta c = c - c_\infty = \Delta c - \Delta c_\infty \tag{6}$$

$$\delta\left(\frac{\alpha}{\omega^2}\right) = \frac{\alpha}{\omega^2} - \left(\frac{\alpha}{\omega^2}\right)_\infty = \frac{\Delta\alpha}{\omega^2} - \left(\frac{\Delta\alpha}{\omega^2}\right)_\infty \tag{7}$$

and the dispersion equations are:

$$-\frac{\delta c}{c^2} = \frac{\rho c\, c_M S}{2kT(1+\omega^2\tau^2)} \tag{8}$$

$$\delta\left(\frac{\alpha}{\omega^2}\right) = \frac{\rho c\, c_M S\,\tau}{2kT(1+\omega^2\tau^2)}. \tag{9}$$

Eqs. 8 and 9 may be rewritten:

$$R' = R'(x) = -\frac{2kT\,\delta c}{\rho c^3\, c_M} = \frac{S}{1+\omega^2\tau^2} \tag{10}$$

$$R'' = R''(x) = \frac{2kT\,\omega\,\delta(\alpha/\omega^2)}{\rho c\, c_M} = \frac{S\,\omega\,\tau}{1+\omega^2\tau^2} \tag{11}$$

and they provide a parametric representation in terms of the variable $x = \omega\tau$ of the Cole-Cole curve $R''(R')$. The quantities R' and R'' are proportional to $-\delta c/c^2$ and $\omega\,\delta(\alpha/\omega^2)$, respectively, with the proportionality factor $\gamma = 2kT/(\rho c\, c_M)$.

For n nonidentical relaxation processes we write Eqs. 12 and 13, instead of Eqs. 10 and 11:

$$R' = \sum_{j=1}^{n} \frac{S_j}{1+\omega^2\tau_j^2} \tag{12}$$

$$R'' = \sum_{j=1}^{n} \frac{S_j\,\omega\,\tau_j}{1+\omega^2\tau_j^2} \tag{13}$$

and any of the $\omega\tau_j$'s may be chosen as the parametric variable x.

For a single relaxation process, the Cole-Cole diagram, as is known, is a half-circle ($R'' > 0$) of equation:

$$\left(R' - \frac{S}{2}\right)^2 + R''^2 = \frac{S^2}{4}. \tag{14}$$

The circle is centered on the R'-axis and its diameter is equal to S. This diagram is represented in Fig. 1, where the points $\omega\tau = 0$, 1 and ∞ are shown.

When several relaxation processes are present, if the highest and lowest relaxation times are each well separated from all other times, i.e., if:

$$\tau_1 \gg \tau_2 > \ldots > \tau_{n-1} \gg \tau_n$$

the Cole-Cole curve approaches half-circles at both ends of the frequency-scale. When $\omega\tau_2 \ll 1$, Eqs. 12 and 13 indeed reduce to Eqs. 15 and 16:

$$R' = \sum_{j=2}^{n} S_j + \frac{S_1}{1+\omega^2\tau_1^2} \tag{15}$$

$$R'' = \frac{S_1\,\omega\tau_1}{1+\omega^2\tau_1^2} \tag{16}$$

so that:

$$\left(R' - \sum_{j=2}^{n} S_j - \frac{S_1}{2}\right)^2 + R''^2 = \frac{S_1^2}{4}. \tag{17}$$

Similarly, for $\omega\tau_{n-1} \gg 1$, the sums in Eqs. 12 and 13 reduce to their nth term, and:

$$\left(R' - \frac{S_n}{2}\right)^2 + R''^2 = \frac{S_n^2}{4}. \tag{18}$$

The zero-frequency point:

$$R' = \sum_{j=1}^{n} S_j = S \tag{19}$$

here gives the sum S of the normal-mode factors S_j, and for a unimolecular process, in an aqueous medium, S is again the sum of volume fluctuations per molecule (14).

Theoretical curves are shown for two relaxations in Fig. 2. The slowest relaxation is numbered 1, and the theoretical curves are drawn for the values of S_j, shown in Table 1, that give the best fit to the experimental data for chymotrypsin (see the following section). The parametric variable is $x = \omega\tau_1$, where τ_1 is the slowest relaxation time. Each curve in Fig. 2 corresponds to a value of $p = \tau_2/\tau_1$.

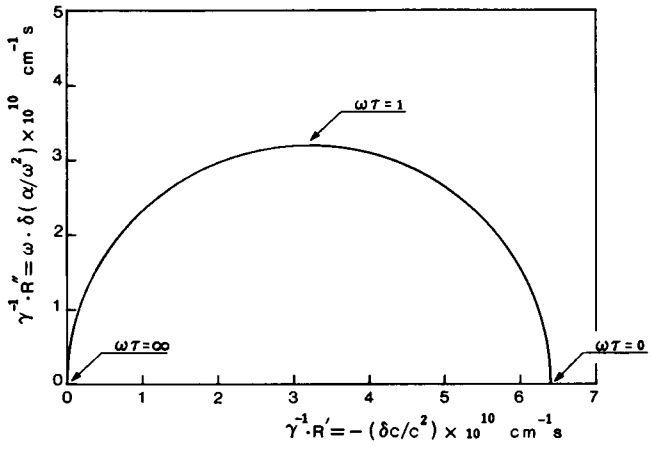

FIGURE 1 Acoustic Cole-Cole diagram for a single-relaxation process. The proportionality factor γ is defined in the text.

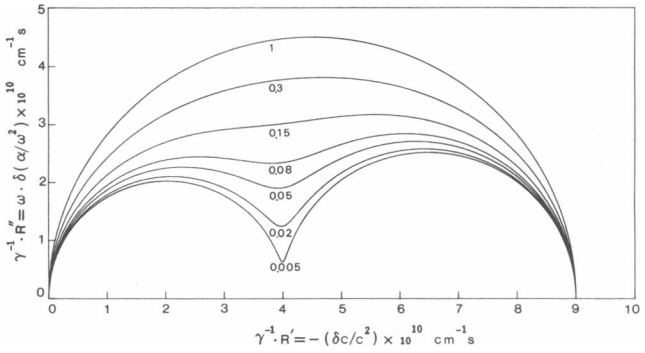

FIGURE 2 Acoustic Cole-Cole diagram for two relaxation processes. The values of S_1 and S_2 are those given in Table I, last row, for a solution of α-chymotrypsin. The values of $p = \tau_2/\tau_1$ are shown in the Figure.

APPLICATION TO α-CHYMOTRYPSIN

Ultrasonic absorption-values α of solutions, and α_0 of solvents were measured using an Eggers resonator (15) between 0.5 and 5.5 MHz, and a pulse technique between 25 and 95 MHz. Ultrasonic velocities were measured between 0.5 and 70.2 MHz using a phase comparison method (16).

All solutions were degassed before measurement, chymotryptic activity was checked after each ultrasonic measurement by following the course of *N*-succinyl-*L*-phenylalanine *p*-nitroanilide hydrolysis, according to Bieth et al. (17).

In Fig. 3 α/N^2 is shown for a 2×10^{-4} M solution of α-chymotrypsin in a 1/15 M phosphate solvent, pH = 7.3, at 25°C (*filled circles*) and for the solvent (*open circles*). Fig. 4 shows the velocity of the waves c to within an additive constant for the same solution (*filled circles*) and for the solvent (*open circles*). The following estimates were made for the high-frequency values of α/N^2 and of Δc:

$$\left(\frac{\alpha}{N^2}\right)_\infty = 25.5\ 10^{-17}\ \mathrm{s^2\ cm^{-1}}$$

$$(\Delta c)_\infty = 21.5\ \mathrm{cm\ s^{-1}}.$$

In Fig. 3 the best fit of two relaxations to the α/N^2 values (continuous line) is also shown. The relaxation times τ_1 and τ_2 and the amplitude factors S_1 and S_2 are given in the first row of Table 1. Similarly, in Fig. 4 the best fit of two relaxations to the velocity data (continuous line) is shown. The corresponding parameter values are given in the second row of Table 1.

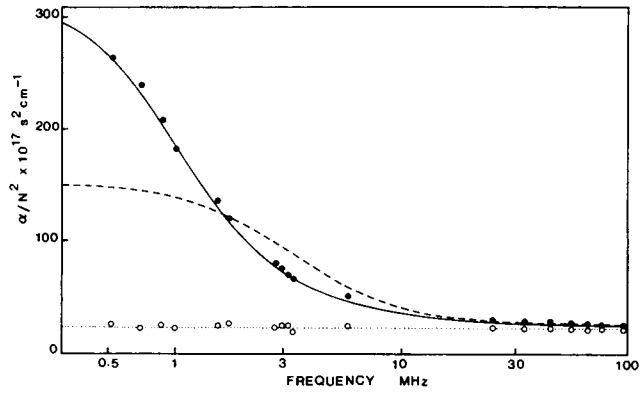

FIGURE 3 Values of α/N^2 for a 2×10^{-4} M solution of α-chymotrypsin in a 1/15 M phosphate solvent, pH = 7.3 at 25°C (*filled circles*) and for the solvent (*open circles*). The continuous line is theoretical for two relaxations. The broken line is transformed from the velocity data of Fig. 4 (see text). The dotted line is hand-drawn for the buffer.

TABLE 1 Parameters derived by deconvolution of ultrasonic data in chymotrypsin solutions

	τ_1	τ_2	S_1	S_2
		MS		*cc/mol²*
Absorption only	0.15	0.008–0.016	725	1,250–626
Velocity only	0.053	0.016	873	393
Cole-Cole	0.13	0.010	824	660

Parameters are derived by using: (*a*) the ultrasonic absorption data only; (*b*) the ultrasonic velocity data only; (*c*) the Cole-Cole representation of both sets of data. In the third row, τ_1 represents the average value τ_{1m} defined in the text.

From these parameter values, that stem from the velocity data, an absorption curve was calculated, using Eqs. 8 and 9, but written with two relaxation terms. The result is shown in Fig. 3 as a broken line. Similarly, in Fig. 4 the broken line shows the velocity curve transformed from the absorption data of Fig. 3, using the parameter values given in the first row of Table 1.

Clearly, the fitting of two relaxations to either only the absorption or only the velocity data leads to errors in the parameter values.

In Fig. 5, each experimental point corresponds to a measured value of α, at a frequency N. When the velocity δc was not available at the same frequency, the value of δc at this frequency N was determined by interpolation between values of δc, measured for two values of the frequency near to N.

The Cole-Cole curve of Fig. 5 was obtained using the following procedure. Two relaxations were assumed, and approximate values of S_1, S_2, and of $p = \tau_2/\tau_1$ were estimated from the experimental plot, remembering that $S_1 + S_2$ is equal to the total length of the Cole-Cole curve and that the maxima of the curve are obtained for ω close to τ_1^{-1} and τ_2^{-1}, respectively.

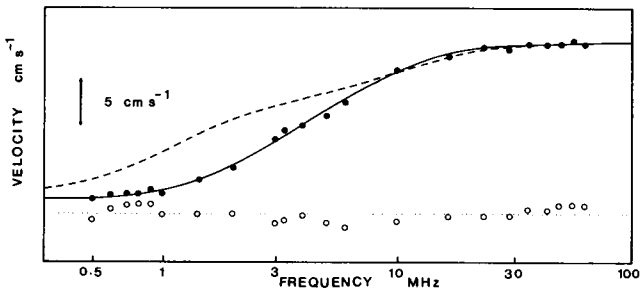

FIGURE 4 Velocity of propagation of ultrasonic waves c to within an additive constant. Conditions are the same as in Fig. 3. The filled circles are for the solution of α-chymotrypsin; the open circles are for the solvent. The continuous line is theoretical for two relaxations. The broken line is transformed from the absorption data of Fig. 3 (see text).

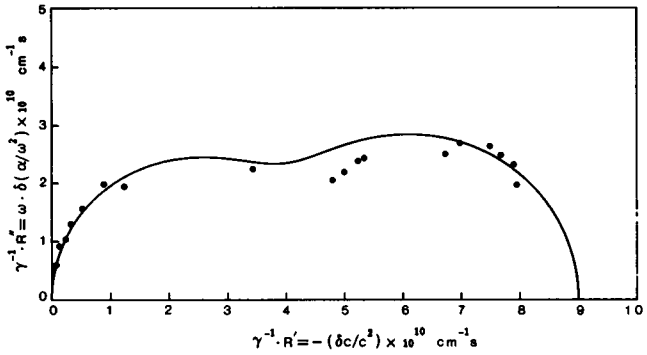

FIGURE 5 Experimental ultrasonic Cole-Cole diagram for α-chymotrypsin solution under the same conditions as in Figs. 3 and 4. Theoretical curve is for two relaxations and for the parameter values of Table I, last row.

Equating the experimental and calculated values of $-\delta c/c^2$ then resulted in a value of $x = \omega\tau_1$, thus of τ_1, for each experimental point in Fig. 5. The mean value τ_{1m} of τ_1 and the normalized standard deviation σ_τ of τ_1 were determined; τ_2 was obtained from the values of τ_1 and p. The normalized standard deviation σ_α of $\omega\,\delta(\alpha/\omega^2)$ was also calculated, and so the parameter values could be improved by optimization. Consideration of σ_α alone would lead to a value of p closer to 0.05 than to 0.08 (compare Figs. 2 and 5). The consideration of σ_τ and σ_α, however, leads to the results shown in Fig. 5 and in Table 1, last row, in which the value of τ_1 is the average value τ_{1m} of the slow relaxation time.

The parameter values determined from the Cole-Cole diagram are seen to represent well both the data for the absorption (Fig. 6) and for the velocity (Fig. 7). The remaining discrepancies that are observed between the

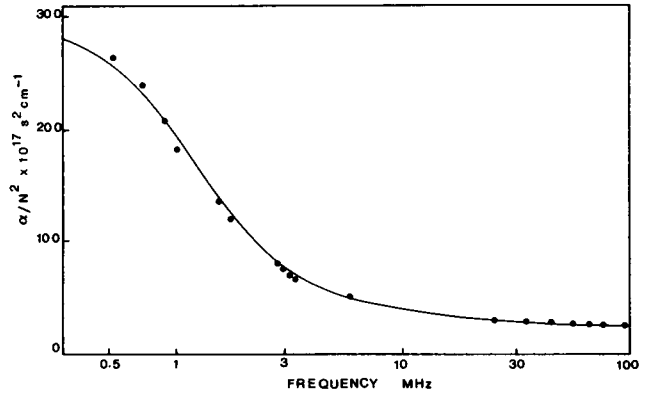

FIGURE 6 Same α/N^2 values as in Fig. 3. The continuous line is theoretical for the parameter values of the last row of Table I (Cole-Cole values).

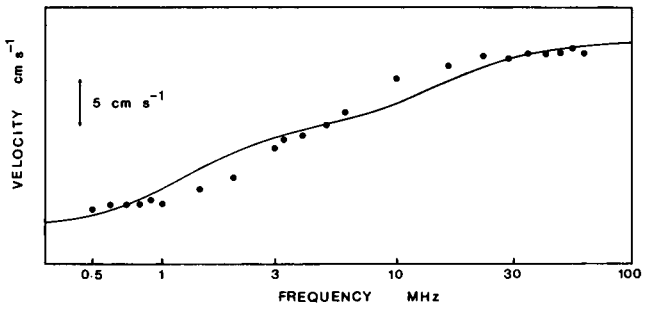

FIGURE 7 Same values of the velocity as in Fig. 4. The continuous line is theoretical for the parameter values of the last row of Table I (Cole-Cole values).

calculated and experimental values of the velocity in Fig. 7 cannot be removed by the consideration of additional relaxations. Adding relaxations, indeed, would result in increasing the discrepancy between calculated and experimental values in the Cole-Cole diagram of Fig. 5.

Rather, those discrepancies are likely to manifest systematic measurement errors. Thus, at frequencies between 1 and 3 MHz the measured velocity seems too low by ~2 cm s^{-1} in Fig. 7. One can then notice that a higher value of the velocity in this range of frequencies is also required to improve the agreement between the measured and calculated values in the Cole-Cole diagram of Fig. 5[1].

CONCLUSIONS

The parameters for the high frequency relaxation, τ_2 and S_2, are poorly determined from absorption measurements only, as shown by the first row of Table 1. Moreover, the preceding discussion has shown that the accuracy of velocity measurements still needs to be improved.

Nevertheless, in combining both the absorption and velocity data in a Cole-Cole diagram, improved parameter values were obtained, as shown by the fits in Figs. 6 and 7.

In view of further studies of α-chymotrypsin in solution, two conclusions are worth noting. (*a*) Only two relaxations are in evidence in the frequency range that was investigated. These relaxations are well separated on the time scale ($\tau_1/\tau_2 > 10$). (*b*) In the example considered

[1]Between 6 and 20 MHz the measured velocity is in excess compared with the calculated value in Fig. 7. These frequencies, however, are between the ranges of our Eggers and pulse devices; therefore no experimental point is available for those frequencies in the Cole-Cole diagram of Fig. 5.

here, the errors on τ_1 and S_1 from absorption measurements are <15%, as shown by comparison of the first and last rows of Table 1. The low frequency relaxation can in this case be fairly well characterized by absorption measurements only.

Received for publication 25 july 1988 and in final form 29 november 1988.

REFERENCES

1. Cerf, R., B. Michels, J. A. Schulz, J. Witz, P. Pfeiffer, and L. Hirth. 1979. Ultrasonic absorption evidence of structural fluctuations in viral capsids. *Proc. Natl. Acad. Sci. USA.* 76:1780–1782.
2. Robach, Y., B. Michels, R. Cerf, J. Braunwald, and F. Tripier-Darcy. 1983. Ultrasonic absorption evidence for structural fluctuations in frog virus 3 and its subparticles. *Proc. Natl. Acad. Sci. USA.* 80:3981–3985.
3. Michels, B., Y. Dormoy, R. Cerf, J. A. Schulz, and J. Witz. 1985. Ultrasonic absorption in tobacco mosaic virus and its protein aggregates. *J. Mol. Biol.* 181:103–110.
4. Cerf, R., and Y. Dormoy. 1986. Ultrasonic absorption evidence for enhanced volume fluctuations in the tobacco mosaic virus protein helical aggregate. *Proc. Natl. Acad. Sci. USA.* 83:8147–8151.
5. Rogez, D., R. Cerf, R. Andrianjara, S. T. Salehi, and H. Fouladgar. 1987. Ultrasonic studies of proton-transfer reactions at the catalytic site of α-chymotrypsin. FEBS (*Fed. Eur. Biochem. Soc.*) *Lett.* 219:22–26.
6. Cerf, R., H. Degermann, and M. Bader. 1970. Mesure précise de petites différences de vitesse de propagation des ultrasons dans les liquides par comparaison de phase, à l'aide d'une cellule tubulaire. *Acustica.* 23:48–49.
7. Rogez, D., R. Cerf, and M. Bader. 1980. Dynamique des chaînes polymériques: mesure différentielle de la vitesse de propagation des ultrasons dans des solutions de polystyrène. *C. R. Acad. Sci. Paris, série B.* 290:377–379.
8. Cole, K. S., and R. H. Cole. 1941. Dispersion and absorption in dielectrics. *J. Chem. Phys.* 9:341–351.
9. Casimir, H. B. G., D. Bijl, and F. K. du Pré. 1941. Measurement on paramagnetic relaxation in chromium potassium alum. *Physica.* 8:449–460.
10. Kneser, H. O. 1943. Über den Zusammenhang zwischen Schallgeschwindigkeit und-absorption bei der akustischen Relaxation. *Ann. der Physik.* 43:465–469.
11. Kneser, H. O. 1961. Schallabsorption und-dispersion in Gasen. In Handbuch der Physik, vol. XI, 1, S. Flügge, editor. Springer-Verlag GmbH & Co., KG, Heidelberg, Germany. 129–201.
12. Litovitz, T. A., and D. Sette. 1953. Dielectric and ultrasonic relaxation in glycerol. *J. Chem. Phys.* 21:17–22.
13. Labbardt, A., and G. Schwarz. 1976. A high resolution and low volume ultrasonic resonator method for fast chemical relaxation measurements. *Berichte der Bunsen Gesellschaft.* 80:83–92.
14. Cerf, R. 1985. Absolute measurement of enhanced fluctuations in assemblies of biomolecules by ultrasonic techniques. *Biophys. J.* 47:751–756.
15. Eggers, F. 1967/68. Eine Resonatormethode zur Bestimmung von Schallgeschwindigkeit und Dämpfung an geringen Flüssigkeitsmengen. *Acustica.* 19:323–329.
16. Rogez, D., and M. Bader. 1984. Ultrasonic velocity dispersion in liquids between 3.3 and 330 MHz using a high resolution phase measurement technique. *J. Acoust. Soc. Am.* 76:167–172.
17. Bieth, J., P. Métais, and J. Warter. 1968. Etude des protéases pancréatiques II—Dosage de la chymotrypsine par la succinyl-phénylalanine-p-nitroanilide et ses applications. *Ann. Biol. Clin.* 26:143–158.